Available online at www.sciencedirect.com
SCIENCE DIRECT
Trans. Nonferrous Met. Soc. China 16(2006) 818−823
Transactions of Nonferrous Metals Society of China
www.csu.edu.cn/ysxb/

Electron beam welding of SiC_p/LD2 composite

CHEN Mao-ai(陈茂爱), WU Chuan-song(武传松), ZOU Zeng-da(邹增大)

Key Laboratory of Liquid Structure and Heredity of Materials, Ministry of Education, Shandong University, Ji'nan 250061, China

Received 18 October 2005; accepted 23 November 2005

Abstract: The 2 mm-thick SiC_p/LD2 composite plates were electron beam welded at different heat inputs. The microstructures of welds were investigated by OM, TEM, SEM, and XRD, and the properties of welds were measured with MTS-810 testing system. The results show that the quantity and size of acicular Al_4C_3 precipitates (interfacial reaction product) decrease with the heat input decreasing. When the heat input lowers to 30 J/mm, the formation of needle-like Al_4C_3 can be prevented. The distributions of SiC in the fusion zones are more uniform than that in as-received composite. TEM analysis reveals that there are Al_4C_3 crystals on the surface of every survived particle, the needle-like Al_4C_3 observed under the optical microscope consists of many tabular Al_4C_3 crystals which have different orientations. With the increase of heat input, the fracture mechanism changes from ductile one to brittle one, the quantity of fractured particles on the fracture face decreases and the strength and ductility of the weld decrease.

Key words: SiC_p/LD2 composite; electron beam welding; interfacial reaction

1 Introduction

SiC particle reinforced aluminum composites (SiC_p/Al) possess excellent properties, e.g. high strength-to-mass ratio, high stiffness-to-mass ratio, good wear resistance and higher service temperature, therefore they are considered a kind of promising structural material. With the gradual reduction in production cost, an increase in uses and application may be expected in the next years. For this reason, welding technologies of this kind of material have attracted a lot of attention recently.

Previous studies reveal that almost all fusion welding processes produce deleterious microstructural alterations when they are applied to SiC_p/Al composites [1−9]. In TIG and MIG welding pool, the strong rejection of SiC particles by solidification front results in microsegregation and inhomogeneous particle distribution, thus reducing the reinforcement efficiency[1−3]. The high hydrogen content in the Al matrix composites (especially the one produced by powder metallurgical routes) and low flowability of molten pool tend to result in serious porosity in both weld and HAZ [2−5]. The vacuum degassing prior to welding can eliminate the porosities in the TIG and MIG welds[2,3,5]. During welding, serious interface reaction between SiC particles and Al matrix occurs and plate-like Al_4C_3 precipitates form, which are very brittle and deleterious to the properties of the weld[2,3,7,8]. However, through applying Al-Si filler metal and/or lowering heat input, the interfacial reaction can be reduced or suppressed[2,3].

By using solid-state joining, the above-mentioned problems can be eliminated. Therefore much more research work has been done in solid-state joining (such as diffusion bonding and friction welding) of SiC particle reinforced aluminum composites and results are encouraging[10−12]. However, the low production efficiency and suitability limit the application fields of those procedures. Thus, it is still necessary to reconsider the possibility of application of the more productive welding processes, fusion welding.

In this paper, the influence of heat input on microstructure and properties of the EB (electron beam) welds in SiC_p/LD2 were studied. The emphasis was placed on the analysis of effect of welding cycle on the particle distribution, Al-SiC interface morphologies and the interfacial reaction products in the welds. The influence of interfacial reaction on the properties and fracture mechanism of the EB welds were also discussed. The mechanism of interfacial reaction was also reviewed.

Foundation item: Project(2004BS05010) supported by Shandong Youth Doctoral Foundation, China
Corresponding author: CHEN Mao-ai; Tel: +86-531-88392711; E-mail: chenmaoai@sdu.edu.cn

2 Experimental

2.1 Material

The material used in this investigation was 2 mm thick plate of SiC particle reinforced LD2 aluminum (SiC_p/LD2). The volume fraction of SiC particle was 10%.

2.2 Welding machine and procedure

The 2 mm thick as-received plate was cut into to-be-welded pieces with 500 mm in length and 50 mm in width. Before welding, the pieces were cleaned with acetone thoroughly to eliminate dirt and grease. Welding experiments were performed with EBW2100/15-150CNC. The welding parameters are listed in Table 1. Heat inputs in Table 1 were calculated as the product of accelerating voltage and beam current divided by traveling speed.

2.3 Microstructure analysis and mechanical testing

Metallurgical specimens were sectioned from the weldment in transverse to the welding direction. The specimens were first polished with diamond paste and water, and finally polished with diamond paste and alcohol to prevent Al_4C_3 that may be present in the weld from decomposing. After polishing, the specimens were cleaned with acetone. Prepared specimens were observed with Neophto-20 optical microscope. Quantitative metallography was used to measure the mean size of Al_4C_3 in individual weld. X-ray diffraction was performed by D/max-rc diffractometry on the specimens sectioned from the top of the weld along the welding direction. The Al-SiC interface morphology in weld metal was examined with H-800 transmission electron microscope. And the fracture surface was examined with Philips-515 scanning electron microscope. The tensile testing was performed on MTS-810 testing system.

3 Results and discussion

Fig.1 shows the typical microstructures of the EB welds in SiC_p/LD2 made at different heat inputs. In the weld made at a heat input of 30 J/mm, the fusion zone microstructure mainly consists of SiC and Al matrix (Fig.1(a)). The Al matrix possesses a very fine cellular solidification structure (3 to 4 μm apparent cell spacing) because of high cooling rate. Compared with the particles in the as-received composite, the surface of survived SiC particle in the fusion zone is much coarser. This suggests that dissolution of SiC particle occurs during welding even at a heat input of 30 J/mm.

In the weld made at a heat input of 36 J/mm, some small-sized needle-like precipitates are observed only in the top center (Fig.1(b)) of the fusion zone. X-ray diffraction analysis indicates that the needle-like precipitates are Al_4C_3. Similar precipitates are also observed in TIG and MIG weld of SiC_p/6061Al and this phase is considered to be deleterious to the properties of material[2−4]. Those precipitates are products of the following interfacial reaction between SiC and molten Al[1, 2]:

$$4Al+3SiC \rightarrow Al_4C_3+3Si$$

The average length of the needle-like Al_4C_3 in the 36 J/mm fusion zone is 6−7 μm. Most of the Al_4C_3 precipitates lie around the survived SiC and some of them are continuous with the survived SiC particles.

In the weld made at a heat input of 42 J/mm, Al_4C_3 precipitates are observed in the whole fusion zone. The number and average size of needle-like Al_4C_3 decrease with the distance from the top center of the fusion zone. The Al_4C_3 needles are randomly oriented (Fig.1(c)). Their average length are about 20 μm. When the heat input increases to 48 J/mm, the average length of needle-like Al_4C_3 increases to about 30 μm, and forms interconnected networks and the number and the size of survived particles decrease (Fig.1(d)). It is apparent from Fig.1 that the amount and size of needle-like Al_4C_3 vary with the heat input. A high heat input results in heavy dissolution of SiC and more and larger Al_4C_3 precipitates. By controlling the heat input, it is possible to avoid the formation of needle-like Al_4C_3.

TEM observation indicates that tabular phases exist at the interface between every survived SiC and Al. Fig.2 shows a typical TEM micrograph of SiC-Al interface in the 30 J/mm fusion zone. The electron diffraction pattern indicates that these phases are Al_4C_3 crystals. This suggests that even welding at a heat input of 30 J/mm, slight interfacial reaction does occur, although no needle-like phases are observed under optical microscope. It can

Table 1 Welding parameters

Weld No.	Accelerating voltage/V	Beam current/A	Focusing current/A	Traveling speed/(mm·s^{-1})	Heat input/(J·min^{-1})
1	150	5	350	25	30
2	150	6	350	25	36
3	150	7	350	25	42
4	150	8	350	25	48

be seen that the tabular Al_4Cl_3 precipitates disperse along the surface of the SiC particles rather than form a continuous layer around SiC. Generally, most of Al_4C_3 tablets form on the surface of the SiC particle and grow into the Al region at the same geometric direction (Fig.2(a)), while some Al_4C_3 rods grow into the SiC particles (Fig.2(b)). Considering that the diffusion rate of Al in solid SiC is very slow. It can be concluded that the Al_4C_3 forms through the following steps: 1) dissolving of SiC in liquid Al and thus generating of Si and C; 2) formation of Al_4C_3 near the interface. The dissolution of the interior part of the SiC particles results from the crystal structure defects.

TEM analysis also reveals that needle-like Al_4C_3 precipitates observed under optical microscope consist of a lot of discrete Al_4C_3 tablets (Fig.3(a)). These tabular Al_4C_3 precipitates have different crystal orientations (Fig.3(b)), although they nearly have the same geometric direction.

The interfacial reaction products between SiC and Al include Al_4C_3 and free Si, but no Si crystals are found at the SiC-Al interface. While equiaxed Si crystals, in single or a group, are observed in the Al region (Fig.4(a)). Other researchers[5,6] also did not found Si on the SiC surface while studying the interfacial products of SiCp/Al composites with TEM or HREM. Those observations suggest that Si produced by interfacial reaction have diffused into the Al matrix at a high rate. In addition, Al-Fe-Si phases are found on the grain boundary of Al in the EB weld (Fig.4(b)).

Fig.5 shows the particle distributions in EB welds and as-received SiC_p/LD2 composite. The particles in the

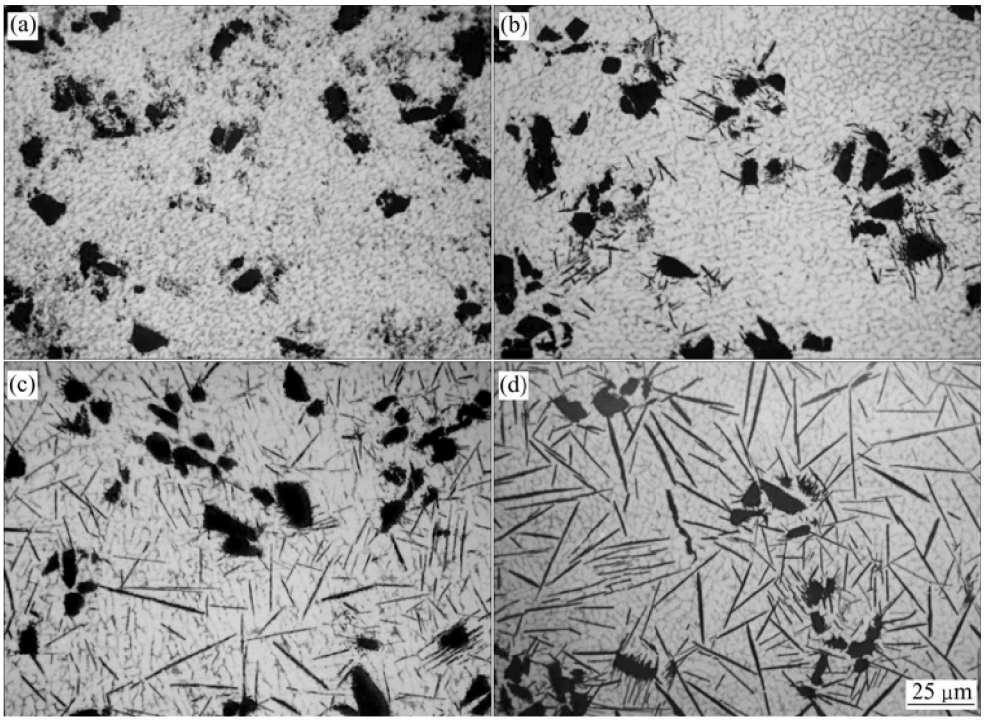

Fig.1 Typical microstructures of EB welds in SiC_p/LD2 made at different heat inputs: (a) 30 J/mm; (b) 36 J/mm; (c) 42 J/mm; (d) 48 J/mm

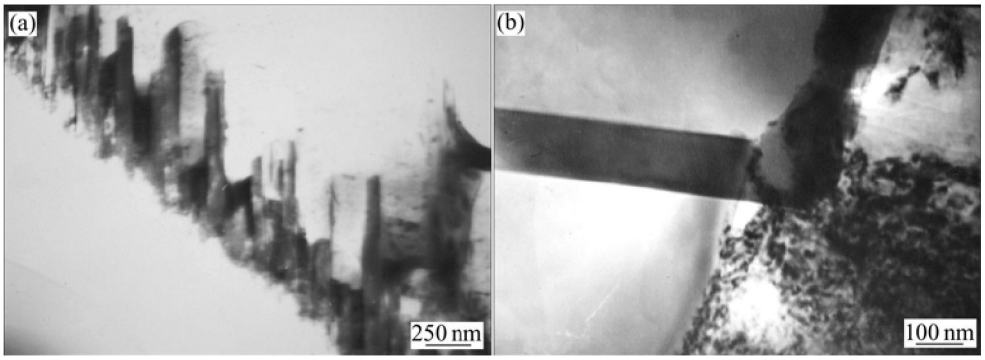

Fig.2 TEM images of SiC-Al interface in 30 J/mm fusion zone: (a) Al_4C_3 tablets growing into Al region; (b) Al_4C_3 tablets growing into SiC particle

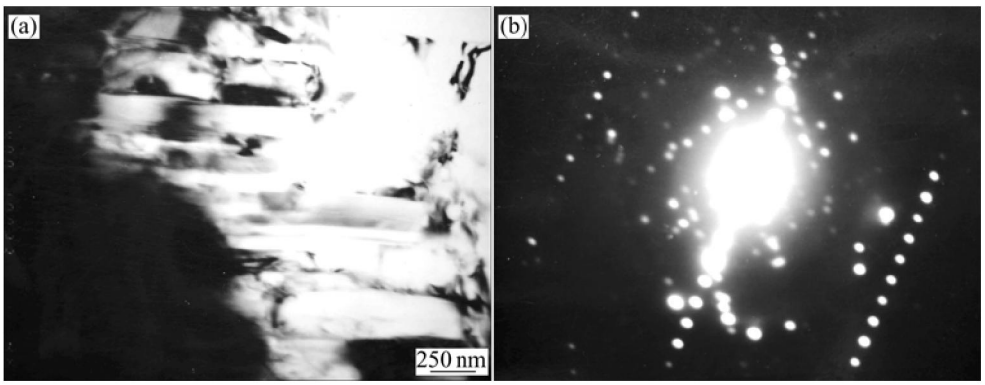

Fig.3 TEM morphologies of needle-like Al_4C_3 in 42 J/mm fusion zone and its diffraction pattern: (a) TEM morphology of needle-like Al_4C_3; (b) Diffraction pattern

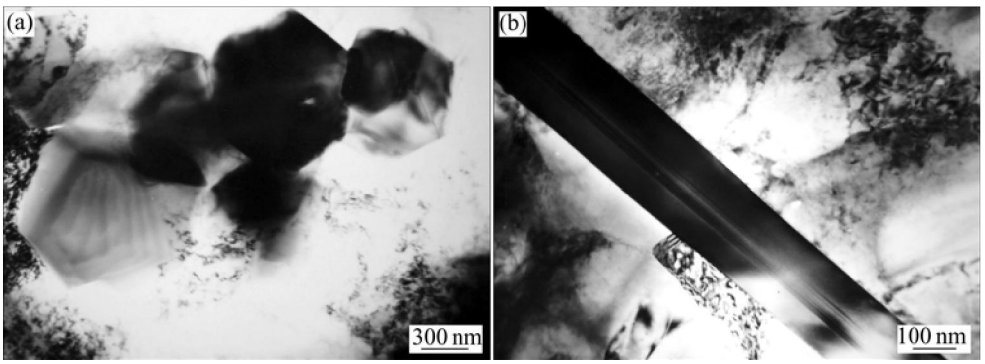

Fig.4 Si crystals (a) and Al-Fe-Si phase (b) in Al region

as-received composite exhibit a slight laminar distribution along the rolling direction (Fig.5(a)). And the SiC particles in the EB weld are distributed much more uniformly (Figs.5(b) and 5(c)). The uniform distribution of particle in weld may be attributed to the key-hole effect and the rapid cooling rate of the EB pool. During welding, the vaporizing of Al matrix and colliding of the atom to the composite result in a formation of keyhole. The melted Al around the keyhole is subjected to a violent stirring movement which might make the SiC particles distribute uniformly in the weld pool. The particle distribution in weld depends on the particle distribution in molten pool and the rejection of the solidification. It is generally accepted that solidification rate influences the rejection effect of solidification front to the particle. As the solidification rate increases, the rejection effect decreases[15]. According to the estimation of Loloyd, the cooling rate of the EB welds is in the range of approximate 3 000−6 000 ℃/s at a heat input of 33.5 J/mm[16]. With such a high cooling rate, almost no particle rejections exist, as a result, the particle distributions in the EB fusion zones are fairly uniform.

Hydrogen porosities often observed in TIG welds and MIG welds are not found in the fusion zone of the EB welds. The possible reason may be as follows: the hydrogen in the molten pool can escape easily because of the vacuum environment of EB welding and the violent stirring of the molten pool; furthermore, no cracks are observed in the EB welds due to the rapid cooling of molten pool.

When welded at a heat input of 30 J/mm, the work-pieces were not completely penetrated, therefore no mechanical property tests were carried out for the 30 J/mm weld. All other weldments were tested under as-welded condition, and failed in the weld metal during testing. The maximum tensile strength measured is about 60% of the as-received composite strength, the maximum elongation is about 40% of the as-received composite elongation. This indicates that the interfacial reaction exerts more effect on the ductility than on the tensile strength. The tensile testing data for individual EB weld are summarized in Table 2. It can be seen from Table 2 that the tensile strength and ductility (elongation) decrease with the heat input increasing

During tensile fracture of SiC_p/Al composite, the crack propagation path involves SiC particles, Al matrix and particle-matrix interface[17]. SEM examination of different fracture surfaces shows that the extent of ductile dimpling decreases with the heat input increasing and the failure mechanism varies with the heat input. Fig.6 shows

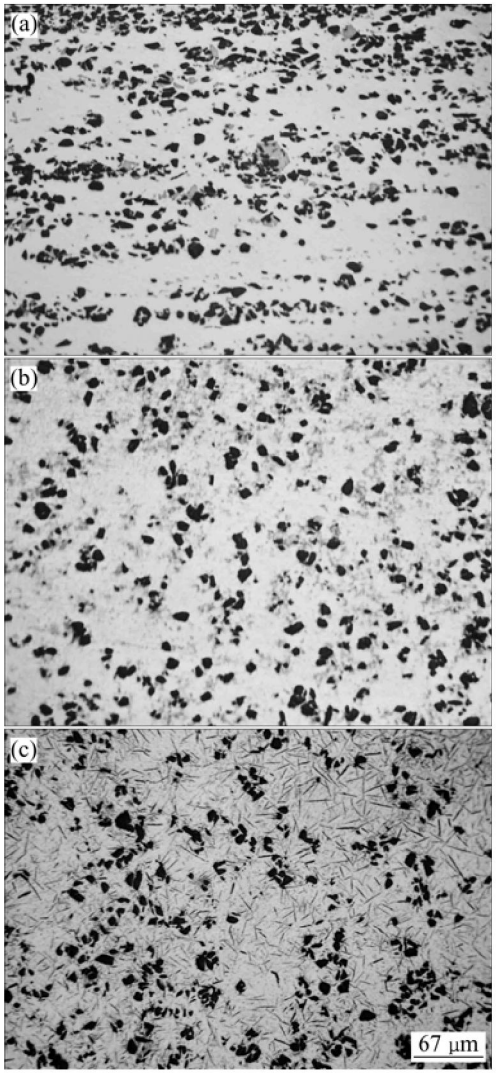

Fig.5 Particle distributions in EB welds and as-received composite: (a) As-received composite; (b) 30 J/mm EB weld; (c) 42 J/mm EB weld

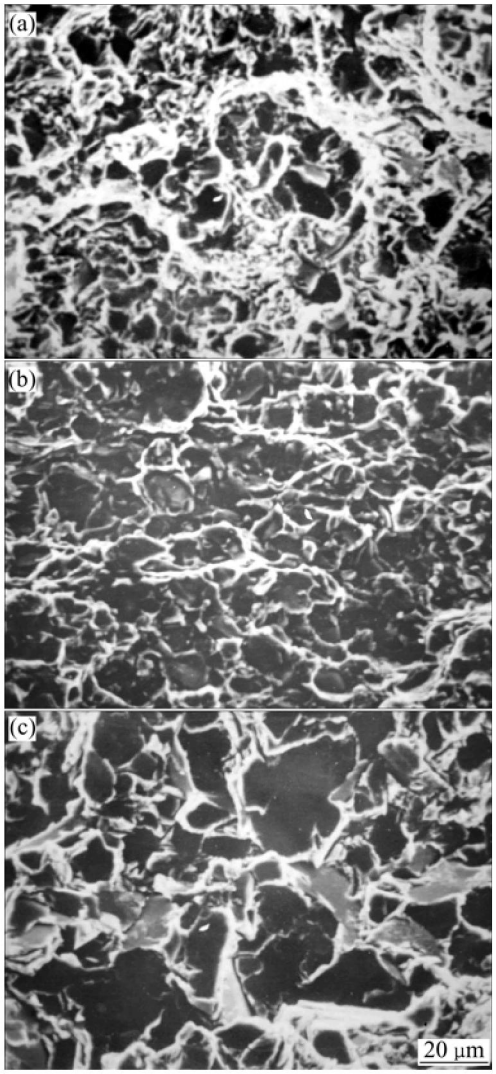

Fig.6 SEM fractographs of EB welds metal and as-received composite: (a) As-received composite; (b) 36 J/mm weld; (c) 48 J/mm weld

Table 2 Tensile Properties of EB welds on SiC_p/LD2

Serial No.	Heat input/ ($J \cdot mm^{-1}$)	Tensile strength/ MPa	Elongation/ %	Remark
0	As-received composite	303	5.6	T6
1	30	–	–	Incomplete penetration
2	36	204	2.1	As-welded
		198	2.3	
		196	2.6	
3	42	169	1.3	As-welded
		153	1.4	
		160	1.6	
4	48	120	–	As-welded
		112	–	
		107	–	

the typical fracture morphologies of as-received composite and individual EB welds. The fracture surface of the as-received composite exhibits typical ductile morphology with a lot of fine dimples in the Al matrix region between particles, there are some fractured particles on the fracture surface (Fig.6(a)). This indicates that the fracture process of as-received material is controlled mainly by matrix ductile failure and particle fracture mechanism.

The fracture surface of the 36 J/mm weld also exhibits evident ductile morphology, the quantity of dimples is much less than that of as-received composite. Although most particles survive the welding cycle, few fractured particles are observed on the fracture surface (Fig.6(b)). This is because that the Al_4C_3 tabular and the dissolution of the SiC surface during welding reduce the strength of SiC-Al interface. The cracks progress along the SiC-Al interface when they meet the particles. In this

case, the weld fracture process is controlled mainly by matrix ductile failure and interface fracture mechanism. The energy required by the crack propagation along the weak interface is much low. Therefore, the strength and elongation of the weld are obviously lower than that of the as-received composite (Table 2), although the particle in the weld is distributed much more uniformly than in the as-received composite.

The fracture surfaces of the 42 J/mm and 48 J/mm welds present typical brittle morphologies in the Al matrix region, and no fractured SiC particles are observed (Fig.6(c)). The corresponding strengths and elongations of the welds are very low (Table 2). The serious interfacial reaction is responsible for the loss of strength and elongation. The formation of network of acicular Al_4C_3 which is very brittle and susceptible to initiate greatly degrades the properties of the weld. Furthermore，another interfacial product, Si, results in brittle aggregates such as Si crystal, Al-Fe-Si intermetallic compound and Al-Cu-Si eutectic on the grain boundary of the Al matrix. Those brittle aggregates degrade the ductility and strength of Al matrix further.

4 Conclusions

1) At all the heat inputs used, interfacial reaction occurs and Al_4C_3 precipitates forms. Both Al_4C_3 tablets growing from interface into the Al region and those growing into the SiC particle are observed. This indicates that Al_4C_3 precipitates can form only after dissolving of SiC in liquid Al.

2) The size and the amount of Al_4C_3 precipitates decrease with the heat input decreasing. When the 2 mm thick SiC_p/LD2 palate is welded at a heat input of 30 J/mm, no needle-like Al_4C_3 precipitates form, SiC particle distribution in EB is more uniform than that in as-received composites. When the heat input increases to 36 J/mm, a few small-sized needle-like precipitates are observed in the top center of the fusion zone, and sound EB welds can be obtained.

3) The needle-like Al_4C_3 precipitate observed under optical microscope consists of many tabular Al_4C_3 crystals which have different orientations.

4) With the heat input increasing, the fracture mechanism changes from ductile one to brittle one, the quantity of fractured particles on the fracture face decreases and the strength and ductility of the weld decrease. The degradation of the properties of the weld are mainly caused by the formation of acicular Al_4C_3 and Si-rich phase.

References

[1] MIDDLING O T, GRONG O. Joining of particle reinforced Al-SiC MMCs [J]. Key Engineering Materials, 1995, 104−107(2): 355−372.

[2] CHEN Mao-ai, WU Chuan-song, GAO Jian-guo. Welding of SiC particle reinforced 6061 Al matrix composite with P-TIG [J]. Trans Nonferrous Met Soc China, 2002, 12(5): 805−808.

[3] CHEN Mao-ai, WU Chuan-song, WANG Jian-guo. Effect of composition of welding wire on microstructure and mechanical properties of weld metal in SiC particle reinforced 6061A1 matrix composite [J]. Transactions of the China Welding Institution, 2003, 24(5): 69−72.(in Chinese)

[4] DEVLETIAN J H. SiC/Al metal matrix composite welding by a capacitor discharge process [J]. Welding Journal, 1987, 66(6): 33−39.

[5] AHEARN J S, COOKE C, FISHMAN S G. Fusion welding of SiC-reinforced Al composite [J]. Metal Construction, 1982, 14(4): 192−197.

[6] NIU Ji-tai, WANG Mu-zhen, LAI Zhong-hong. Mechanism of laser welding for SiC_w/6061Al composite [J]. Transactions of the China Welding Institution, 2000, 21(1): 1−4.(in Chinese)

[7] URENA A, ESCALERA M D, GIL L. Influence of interface reaction on fracture mechanisms in TIG arc-welded aluminum matrix composites [J]. Composites Science and Technology, 2000, 20(4): 613−622.

[8] NARENDRA B, DAHOTRE T, DWAYNE M, MCCAY M H. Laser processing of a SiC/Al alloy metal matrix composite [J]. Journal of Applied Physics, 1989, 65(12): 5072−5077.

[9] LEAN P P, GIL L, URENA A. Dissimilar welds between unreinforced AA6082 an AA6092/SiC/25p composite by P-MIG using unreinforced filler alloys [J]. Journal of Material Processing Technology, 2003, 143−144: 846−850.

[10] FERNANDEZ G J, MURR L Z. Characterization of tool wear and weld optimization in the friction-stir welding of cast Al 359+20% SiC MMC [J]. Material Characterization, 2004, 52(1): 65−75.

[11] NIU Ji-tai, GUO Wei, MENG Qing-chang, ZHANG Bao-you. Diffusion welding SiC_p/ZL101 with Ni interlayer [J]. Journal of University of Science and Technology, 2004, 11(1): 85−89.

[12] ZHANG X P, YE L, MAI Y W, QUAN G F, WEI W. Investigation on diffusion bonding characteristics of SiC particle reinforced aluminum metal matrix composite [J]. Composite, 1999, 30(5): 1415−1421.

[13] JANGHORBAN K. Investigation of the effect of silicon and carbon on the phase composition of SiC/Al composite [J]. Composite and Technology, 1994, 50(2): 299−303.

[14] ISKI T, KAMEDA T, MARUYAMA T, MARUYAMA T. Interfacial Reactions Between SiC and Al during Joining [J]. Journal of Mater Science, 1984, 19(11): 1692−1698.

[15] XIE Guo-hong. Solidification Mechanisms of SiC Reinforced Aluminum Composite [D]. Shanghai: Shanghai Jiaotong University, 1995. 45−48.(in Chinese)

[16] LIENT T J, BRANDON E D, LIPPOLD J C. Laser and electron beam welding of SiC_p/A-356 MMC [J]. Scripta Metallurgica et Materialia, 1993, 28(11): 1341−1346.

[17] LLOYYD D J, LAGACE H, MCLEOD A, MORRIS P L. Microstructure aspects of aluminum-silicon carbide particulate composite produced by a casting method [J]. Mater Science and Engineering, 1989, A107(1): 73−80.

(Edited by LI Xiang-qun)